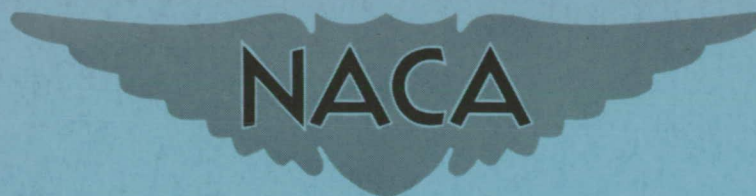


RM L52T26a



# RESEARCH MEMORANDUM

MEASUREMENTS OF AERODYNAMIC HEATING OBTAINED DURING  
DEMONSTRATION FLIGHT TESTS OF THE  
DOUGLAS D-558-II AIRPLANE

By Ira P. Jones, Jr.

Langley Aeronautical Laboratory  
Langley Field, Va.

**NATIONAL ADVISORY COMMITTEE  
FOR AERONAUTICS  
WASHINGTON**

November 26, 1952  
Declassified June 24, 1958

NATIONAL ADVISORY COMMITTEE FOR AERONAUTICS

---

RESEARCH MEMORANDUM

---

MEASUREMENTS OF AERODYNAMIC HEATING OBTAINED DURING  
DEMONSTRATION FLIGHT TESTS OF THE  
DOUGLAS D-558-II AIRPLANE

By Ira P. Jones, Jr.

SUMMARY

During demonstration flight tests of the air-launched Douglas D-558-II airplane, measurements of aerodynamic heating were obtained in flights up to a Mach number of about 1.89 and to an altitude of about 77,000 feet. Measurements were made of stagnation temperature, canopy-glass temperature, and the temperatures of the skin on the nose cone and wing leading edge.

The experimental and theoretical values of the nose-skin and stagnation temperatures show fair agreement through the speed and altitude range tested. The maximum temperatures measured were not great enough to cause any appreciable loss in structural strength for the positions measured.

INTRODUCTION

The National Advisory Committee for Aeronautics is conducting a flight research program utilizing the Douglas D-558-II research airplanes at the NACA High-Speed Flight Research Station at Edwards Air Force Base, Calif. The D-558-II airplanes were designed for flight research in the transonic speed range and were procured for the NACA by the Bureau of Aeronautics, Department of the Navy.

Recently one of the airplanes was modified by the removal of the jet engine and by the installation of larger tanks for increased rocket propellant. The airplane was equipped for air launching so that increased rocket-powered flight time, speed, and altitude could be obtained. The Douglas Aircraft Co. has conducted a flight demonstration of the airplane and its engine. During this demonstration a Mach number of 1.89 and an altitude of about 77,000 feet were obtained.

During the latter portion of this demonstration, the NACA added instrumentation for the purpose of obtaining data on aerodynamic heating of the skin and cockpit canopy glass.

The results of this investigation are presented in the present paper.

### SYMBOLS

$h_p$	pressure altitude, ft
$q$	dynamic pressure, lb/sq ft
$M$	free-stream Mach number
$t$	time, sec
$t_o$	temperature, °F
$T_l$	ambient air temperature, °F abs.
$T_T$	total or stagnation temperature, °F abs.
$T_s$	skin temperature, °F abs.
$T_p$	stagnation temperature measured by probe, °F abs.
$T_{aw}$	adiabatic wall temperature, °F abs.
$\gamma$	ratio of specific heat at constant pressure to specific heat at constant volume (assumed equal to 1.4 for air)
$K$	temperature recovery factor
$G$	heat-absorption capacity of skin, Btu/(sq ft)(°F)
$h$	local effective convective heat-transfer coefficient, Btu/(sec)(sq ft)(°F)
$\epsilon$	emissivity ( $\epsilon = 1$ for perfect black body)
$\gamma_w$	specific weight of skin, lb/cu ft
$c_w$	specific heat of skin, Btu/lb/°F

$\frac{dT_s}{dt}$  slope of measured-skin-temperature curve, deg/sec

$\tau_w$  skin thickness, ft

### DESCRIPTION OF THE AIRPLANE

The D-558-II airplanes were originally constructed to incorporate a combination of turbojet and rocket power. The airplane used in the demonstration was modified for air launching and all-rocket power. The modification made possible an increase in the amount of rocket propellants so that a powered flight of approximately 720 cylinder-seconds was possible. The airplane is powered by a four-cylinder Reaction Motors, Inc., rocket engine which utilizes alcohol-water and liquid oxygen as propellants and has a design thrust of 1500 pounds per cylinder at sea level.

The airplanes have sweptback wing and tail surfaces and are equipped with adjustable stabilizers. Table I presents the pertinent airplane physical characteristics, and figure 1 is a three-view drawing of the airplane. A one-quarter front view is shown as figure 2.

### INSTRUMENTATION

Although the airplane is instrumented to record stability and control, performance, and loads data, only that instrumentation which was used to obtain the aerodynamic-heating data will be discussed here.

The stagnation temperature was measured by use of an NACA standard adiabatic-type resistance bulb thermometer mounted on the exterior of the nose-wheel door outside the fuselage boundary layer. A sketch of the resistance bulb is presented in figure 3 and its position on the airplane is shown in figure 4.

The stagnation-temperature probe has an average recovery factor of 0.992 between Mach numbers of 1 and 2. The time lag of the probe is 0.10 second at 400 miles per hour at sea level. The accuracy of the probe is as good as the accuracy of the film and calibration reading which is  $\pm 1.0^\circ$  F.

Surface temperatures were measured at three points on the airplane. One was on the skin of the nose section forward of the cockpit canopy and below the fuselage center line at fuselage station 32. Another point was located on the skin of the leading edge of the left wing at wing station 52. The remaining measurement was made on the external surface

of the left panel of the cockpit canopy glass. The exact locations and nature of the surrounding structure are shown in figures 4 and 5.

The skin and canopy-glass temperatures were measured with a strain-gage-type wire resistance temperature gage manufactured by Ruge - de Forest, Inc., under the name of RdF Stikon, type BN-1 resistance thermometer element. The gage will operate with full accuracy in continuous service from  $-100^{\circ}$  F to  $3000^{\circ}$  F. The gage has a temperature-time response of approximately  $25^{\circ}$  per second which is considered sufficiently responsive for the conditions tested. The gage wire is bounded to a paper-thin Bakelite wafer. The dimensions of the gage are shown in figure 5. It was possible to mount the temperature gages to the external surface of the skin and still maintain a smooth skin condition which would not change the boundary-layer profile. This was accomplished by removing the thick layer of white lacquer on the skin and inserting the gage in its place and re-covering with a thin coat of white lacquer. The gages were attached to the surfaces by placing a thin coat of 3-M cement on the surface, another coat on the gage, then applying pressure until the cement dried. The canopy gage was glued to the exterior canopy glass. All the temperatures measured were recorded on four channels of a standard NACA 12-element recording galvanometer. The accuracy of the surface-temperature measurements is  $1.0^{\circ}$  F.

The ambient air temperature was determined by the use of a radiosonde balloon which was released just prior to each flight. Ambient air temperatures above the altitude for which radiosonde records were available for the two flights reported were found by using an average of a number of radiosonde records taken at the same season of the year. The records of the radiosonde ambient air temperature are accurate within  $\pm 1.0^{\circ}$  F, neglecting the radiation error. No correction was made to the radiosonde data for radiation error.

The free-stream Mach number used in calculations was obtained from the flight data of a standard NACA airspeed-altitude recorder corrected by the use of radar and radiosonde pressure measurements. An error of  $\pm 0.02$  in Mach number can be expected in supersonic flight.

## CALCULATIONS

### Stagnation-Temperature Probe

The adiabatic-temperature equation relating stagnation and ambient temperature is

$$T_T = T_1 \left( 1 + \frac{\gamma - 1}{2} M^2 \right) \quad (1)$$

The stagnation-temperature-probe equation is

$$T_p = T_1 \left( 1 + \frac{\gamma - 1}{2} M^2 \right) \quad (2)$$

From equation (2) the ambient temperature at any time during the flight can be found from the equation

$$T_1 = \frac{T_p}{\left( 1 + \frac{\gamma - 1}{2} M^2 \right)} \quad (3)$$

Substituting this value for  $T_1$  into the original adiabatic-temperature equation (1) results in

$$T_T = T_p \frac{1 + \frac{\gamma - 1}{2} M^2}{1 + \frac{\gamma - 1}{2} M^2} \quad (4)$$

For the Mach number range covered, the factor  $\frac{1 + \frac{\gamma - 1}{2} M^2}{1 + \frac{\gamma - 1}{2} M^2}$  is very close to unity and the recorded probe temperature may be taken as the true adiabatic stagnation temperature

$$T_T = T_p \quad (5)$$

The theoretical stagnation temperatures for purposes of comparison with the measured stagnation temperature were computed from equation (1) by using standard atmospheric tables for the values of ambient temperature.

#### Theoretical Transient Skin Temperature

In order to check the skin temperatures that were measured on the airplane, a calculation of the transient skin temperature on the nose was made by using two methods of evaluating the heat-transfer coefficient. No instrumentation was available to determine the flow conditions and the local pressure and Mach number at the point of the temperature measurements.

The basic transient-skin-temperature equation is

$$\gamma_w c_w T_w \frac{dT_s}{dt} + hT_s + 4.8 \times 10^{-13} \epsilon T_s^4 = hT_{aw} \quad (6)$$

For the skin temperature encountered in these tests the radiation was negligible; therefore equation (6) reduces to

$$G \frac{dT_s}{dt} + hT_s = hT_{aw} \quad (7)$$

or

$$h = \frac{G \frac{dT_s}{dt}}{T_{aw} - T_s} \quad (8)$$

The first method of calculation uses the measured flight data to determine the heat-transfer coefficient. Before  $h$  can be found from equation (8),  $T_{aw}$  must be evaluated. This is done by solving

$$K = \frac{T_{aw} - T_1}{T_T - T_1} \quad (9)$$

for  $T_{aw}$ . At the peak  $\left(\frac{dT_s}{dt} = 0\right)$  of the skin-temperature curve,  $T_{aw}$  is equal to  $T_s$ , as can be seen in equation (7). Therefore, a value of the recovery factor can be found for this condition. The assumption is made that the value of the recovery factor is constant for the entire flight; therefore  $T_{aw}$  and  $h$  can be evaluated at any time during the flight. A value of 0.84 for the recovery factor on the nose cone was used in the calculations. The experimental heat-transfer coefficient which was found from equation (8) was used in a numerical solution of the simplified transient-skin-temperature equation (7) as presented in reference 1, from which a time history of the transient skin temperature was found.

The second method presented used the empirical formula developed by Eber as given in reference 1 for determining the value of  $h$ . The solution from that point on was the same as the first method.

Only the nose-skin transient temperature was calculated, inasmuch as the solution of the Eber heat-transfer-coefficient equation of reference 1 was for a conical-shaped body. Although the basic shape of the forward portion of the airplane fuselage is an ogive and not a cone, the calculations assumed a conical nose section using an apex angle ( $32^\circ$ ) formed by a tangent line from the temperature gage to the fuselage center line. Additional work on the calculation of surface temperatures at high speed can be found in references 2 to 4.

## RESULTS AND DISCUSSION

The temperature measurements were made during flights to maximum Mach number and maximum altitude. These data should be considered as preliminary because these are the first data obtained with this installation.

Figure 6 shows a time history of stagnation, canopy-glass, wing-skin, and nose-skin temperatures obtained during a flight to a maximum Mach number of 1.89. Figure 7 shows a time history of these temperature measurements during a flight to an altitude above 77,000 feet. Shown in figures 8 and 9 are the measured and computed values for stagnation and nose-skin temperature together with the free-stream dynamic pressure. Figures 8 and 9 show that the computed stagnation and nose-skin temperatures agree fairly well with the measured values. The computations using the experimental heat-transfer coefficients showed closer agreement than did the Eber coefficients. However, based upon these results, use of the Eber empirical heat-transfer coefficients for determining the transient skin temperature will be satisfactory for a first approximation. The accuracy of this method can be improved by obtaining the recovery factor in flight for one condition and then using it with the Eber coefficient to determine the skin temperature under other conditions.

For the flight to maximum Mach number (fig. 6) the maximum nose-skin temperature was  $76^{\circ}$  F which was a maximum temperature rise above the ambient temperature of  $151^{\circ}$  F. The corresponding maximum stagnation temperature was  $199^{\circ}$  F, or a rise of  $273^{\circ}$  F. The high-altitude flight (fig. 7) resulted in much lower temperatures than the flight to maximum Mach number. The temperature rise on the nose skin was  $115^{\circ}$  F and the stagnation temperature rise was  $175^{\circ}$  F. The nose skin reached a temperature of  $41^{\circ}$  F and the maximum stagnation temperature was  $113^{\circ}$  F.

Reference 5 presents data showing the loss in the ultimate and yield tensile stresses at elevated temperatures for aluminum and magnesium alloys. The reference indicates that the temperature increases that were measured were not of sufficient magnitude to cause any loss in structural strength at the positions measured. However, if flight could have been maintained at the maximum Mach number for a longer duration, a stabilized temperature could have been reached which would have caused a loss in the structural strength of certain parts of the airplane. At no time during the flights did the skin temperature approach the equilibrium temperature, since it is apparent from the fact that, during the decelerating part of the flight, the skin temperature was greater than the stagnation temperature. Indications are that the design of the airplane at present is such that a sufficiently high Mach number cannot be maintained long enough to produce an adverse temperature effect on the structure.



## CONCLUSIONS

As a result of the transient aerodynamic-heating measurements on the Douglas D-558-II airplane the following conclusions are made:

1. The transient skin and stagnation temperatures on the nose showed fair agreement between measured and computed values.
2. The maximum temperatures were not great enough to cause any appreciable loss in structural strength at these points.

Langley Aeronautical Laboratory,  
National Advisory Committee for Aeronautics,  
Langley Field, Va.

## REFERENCES

1. Lo, Hsu: Determination of Transient Skin Temperature of Conical Bodies During Short-Time, High-Speed Flight. NACA TN 1725, 1948.
2. Wood, George P.: Calculation of Surface Temperatures in Steady Supersonic Flight. NACA TN 1114, 1946.
3. Scherrer, Richard: The Effects of Aerodynamic Heating and Heat Transfer on the Surface Temperature of a Body of Revolution in Steady Supersonic Flight. NACA Rep. 917, 1948. (Supersedes NACA TN 1300.)
4. Huston, Wilber B., Warfield, Calvin N., and Stone, Anna Z.: A Study of Skin Temperatures of Conical Bodies in Supersonic Flight. NACA TN 1724, 1948.
5. Anon.: Strength of Metal Aircraft Elements. ANC-5, Munitions Board Aircraft Committee, Dept. of Defense. Revised ed., June 1951.

TABLE I.- PHYSICAL CHARACTERISTICS OF THE  
DOUGLAS D-558-II AIRPLANE

## Wing:

Root airfoil section (normal to 0.30 chord) . . . . .	NACA 63-010
Tip airfoil section (normal to 0.30 chord) . . . . .	NACA 063 <sub>1</sub> -012
Total area, sq ft . . . . .	175.0
Span, ft . . . . .	25.0
Mean aerodynamic chord, in. . . . .	87.301
Root chord (parallel to plane of symmetry), in. . . . .	108.51
Tip chord (parallel to plane of symmetry), in. . . . .	61.18
Taper ratio . . . . .	0.565
Aspect ratio . . . . .	3.570
Sweep at 0.30 chord, deg . . . . .	35.0
Incidence at fuselage center line, deg . . . . .	3.0
Dihedral, deg . . . . .	-3.0
Geometric twist, deg . . . . .	0
Total aileron area (aft of hinge), sq ft . . . . .	9.8
Aileron travel (each), deg . . . . .	±15
Total flap area, sq ft . . . . .	12.58
Flap travel, deg . . . . .	50

## Horizontal tail:

Root airfoil section (normal to 0.30 chord) . . . . .	NACA 63-010
Tip airfoil section (normal to 0.30 chord) . . . . .	NACA 63-010
Area (including fuselage), sq ft . . . . .	39.9
Span, in. . . . .	143.6
Mean aerodynamic chord, in. . . . .	41.75
Root chord (parallel to plane of symmetry), in. . . . .	53.6
Tip chord (parallel to plane of symmetry), in. . . . .	26.8
Taper ratio . . . . .	0.50
Aspect ratio . . . . .	3.59
Sweep at 0.30-chord line, deg . . . . .	40.0
Dihedral, deg . . . . .	0
Elevator area, sq ft . . . . .	9.4
Elevator travel, deg	
Up . . . . .	25
Down . . . . .	15
Stabilizer travel, deg	
Leading edge up . . . . .	4
Leading edge down . . . . .	5



TABLE I.- PHYSICAL CHARACTERISTICS OF THE  
DOUGLAS D-558-II AIRPLANE - Concluded

## Vertical tail:

Airfoil section (normal to 0.30 chord) . . . . .	NACA 63-010
Area, sq ft . . . . .	36.6
Height from fuselage center line, in. . . . .	98.0
Root chord (parallel to fuselage center line), in. . . . .	146.0
Tip chord (parallel to fuselage center line), in. . . . .	44.0
Sweep angle at 0.30 chord, deg . . . . .	49.0
Rudder area (aft hinge line), sq ft . . . . .	6.15
Rudder travel, deg . . . . .	±25

## Fuselage:

Length, ft . . . . .	42.0
Maximum diameter, in. . . . .	60.0
Fineness ratio . . . . .	8.40
Speed-retarder area, sq ft . . . . .	5.25

## Power plant:

Rocket . . . . . Reaction Motors, Inc.

Airplane weight (full rocket fuel), lb . . . . . 15,787

Airplane weight (no fuel), lb . . . . . 9,421

## Center-of-gravity locations:

Full rocket fuel (gear up), percent mean aerodynamic chord . .	24.6
No fuel (gear up), percent mean aerodynamic chord . . . . .	27.3
No fuel (gear down), percent mean aerodynamic chord . . . . .	26.7

## Canopy glass:

Glass density, lb/ft <sup>3</sup> . . . . .	157.90
Glass specific heat . . . . .	0.205
Glass thermal conductivity, Btu/ft <sup>2</sup> -hr-°F-ft . . . . .	0.5562
Vinyl density, lb/ft <sup>3</sup> . . . . .	73.55
Vinyl specific heat . . . . .	0.350
Vinyl thermal conductivity, Btu/ft <sup>2</sup> -hr-°F-ft . . . . .	0.121



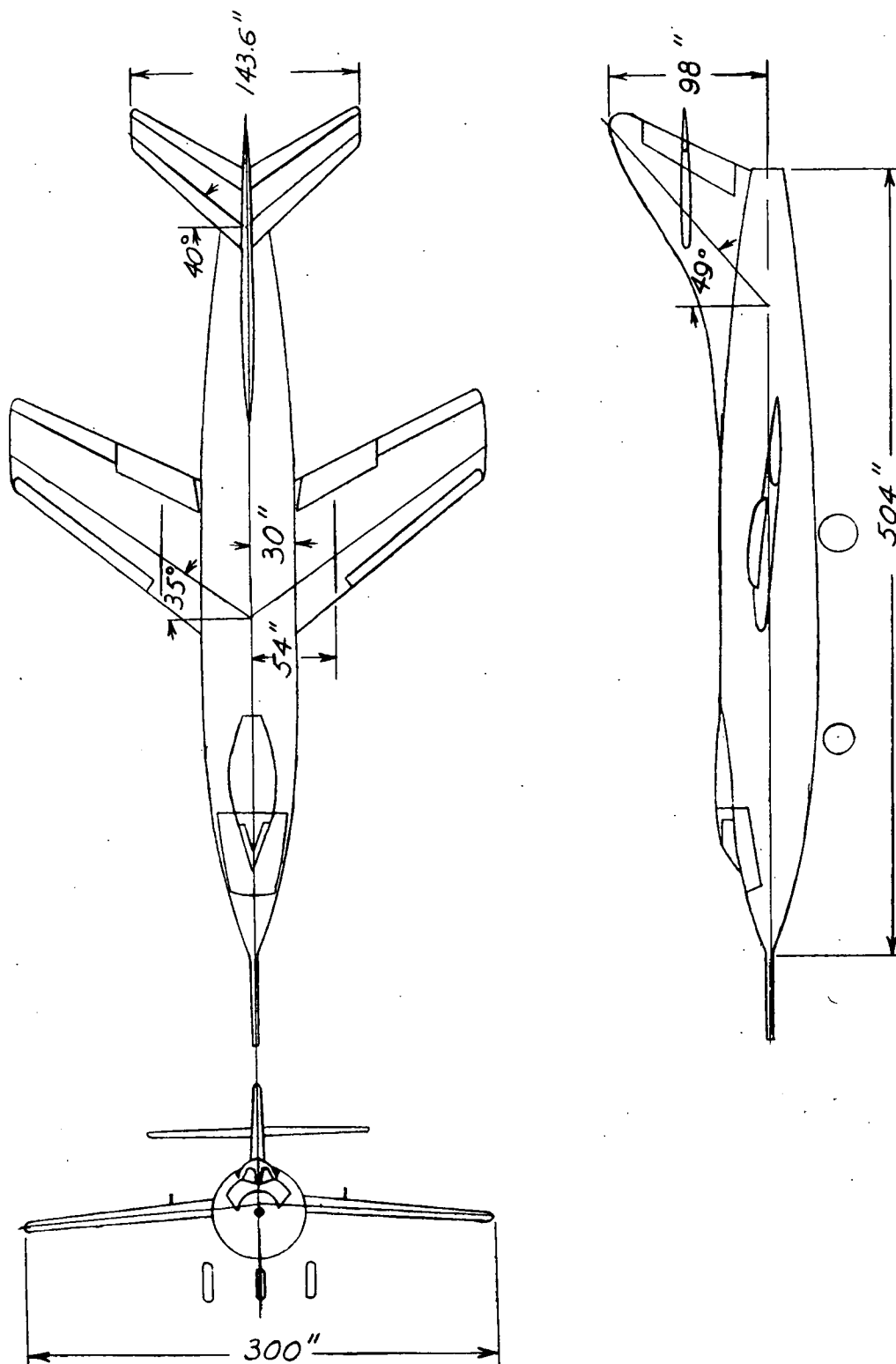


Figure 1.- Three-view drawing of the Douglas D-558-II research airplane.

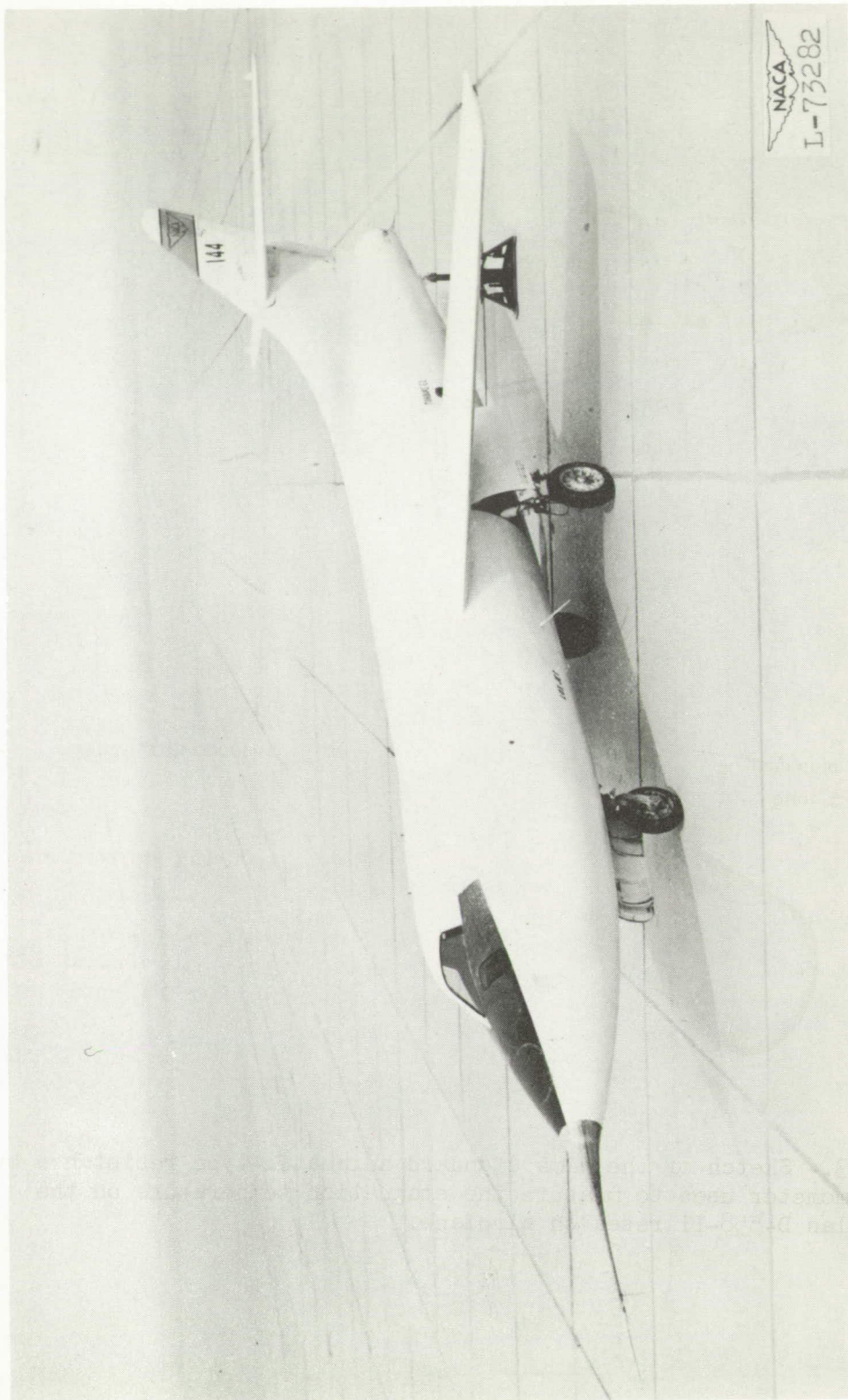


Figure 2.- One-quarter front view of Douglas D-558-II research airplane.

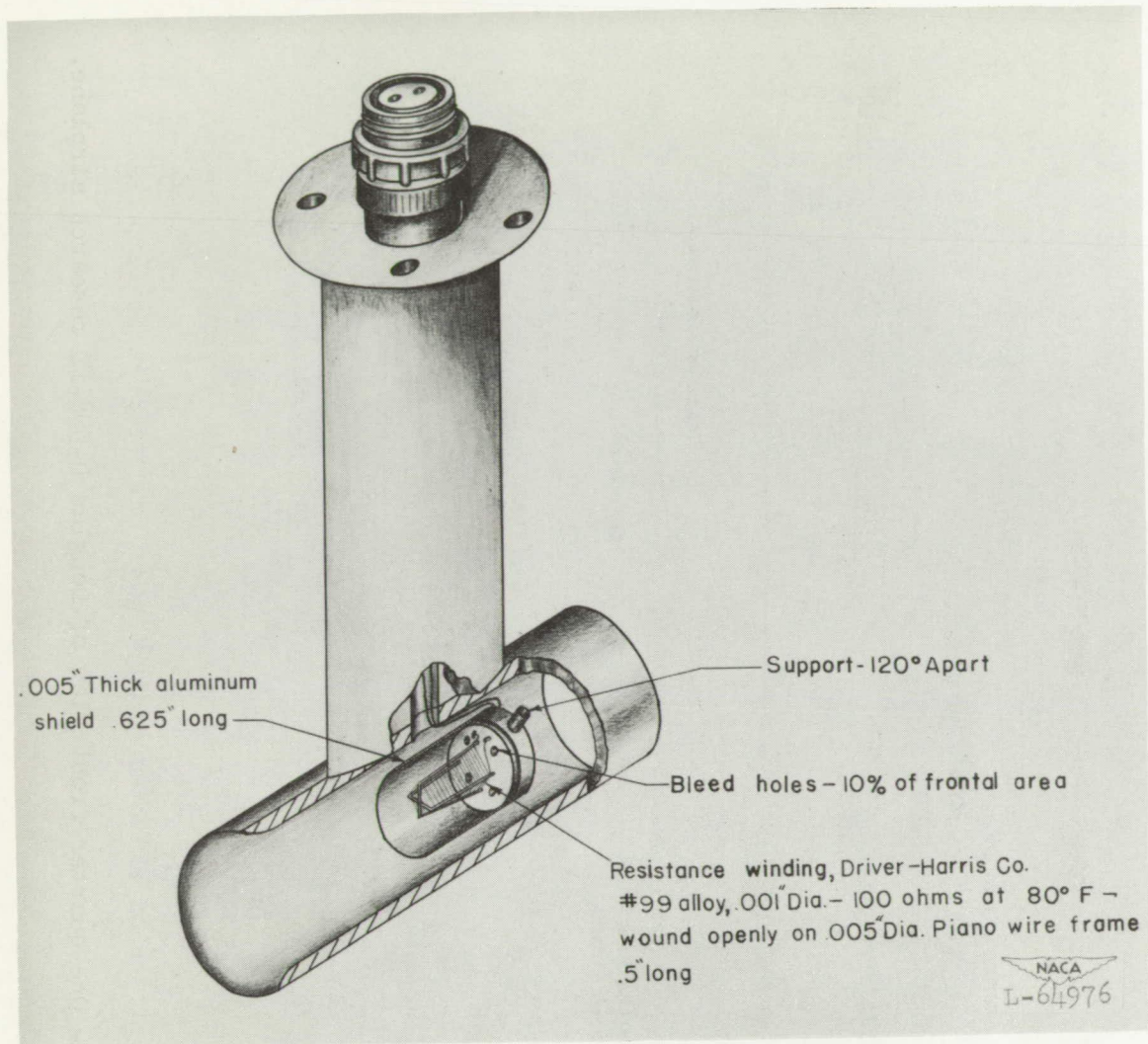


Figure 3.- Sketch of the NACA standard adiabatic-type resistance bulb thermometer used to measure the stagnation temperature on the Douglas D-558-II research airplane.

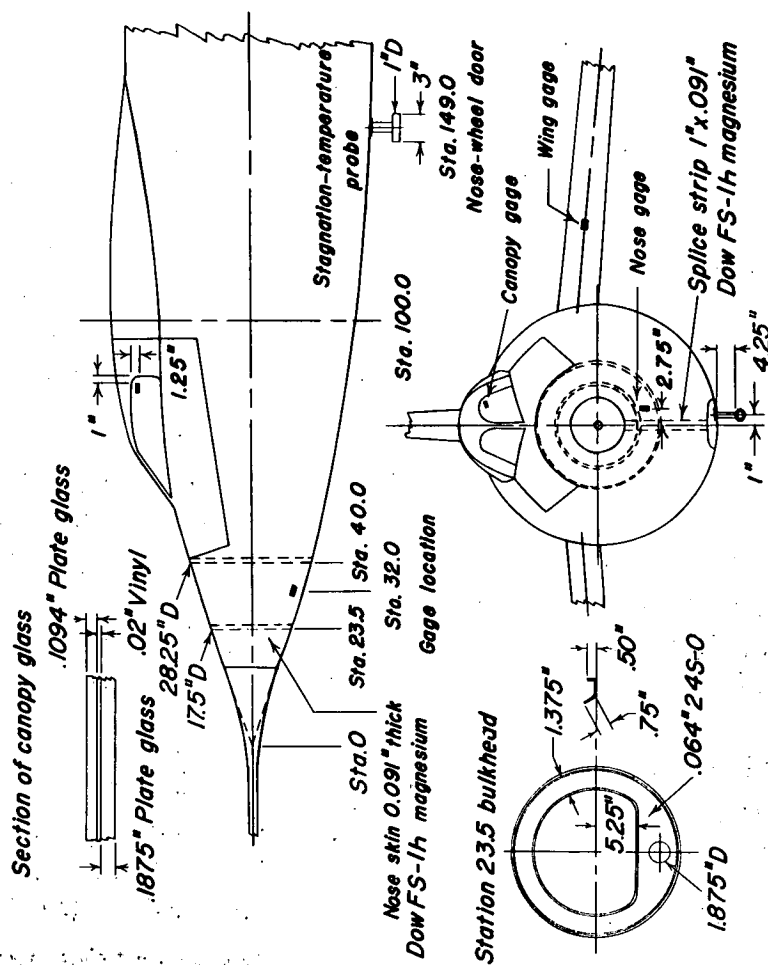


Figure 4.- Position of skin-temperature gages and stagnation-temperature probe.

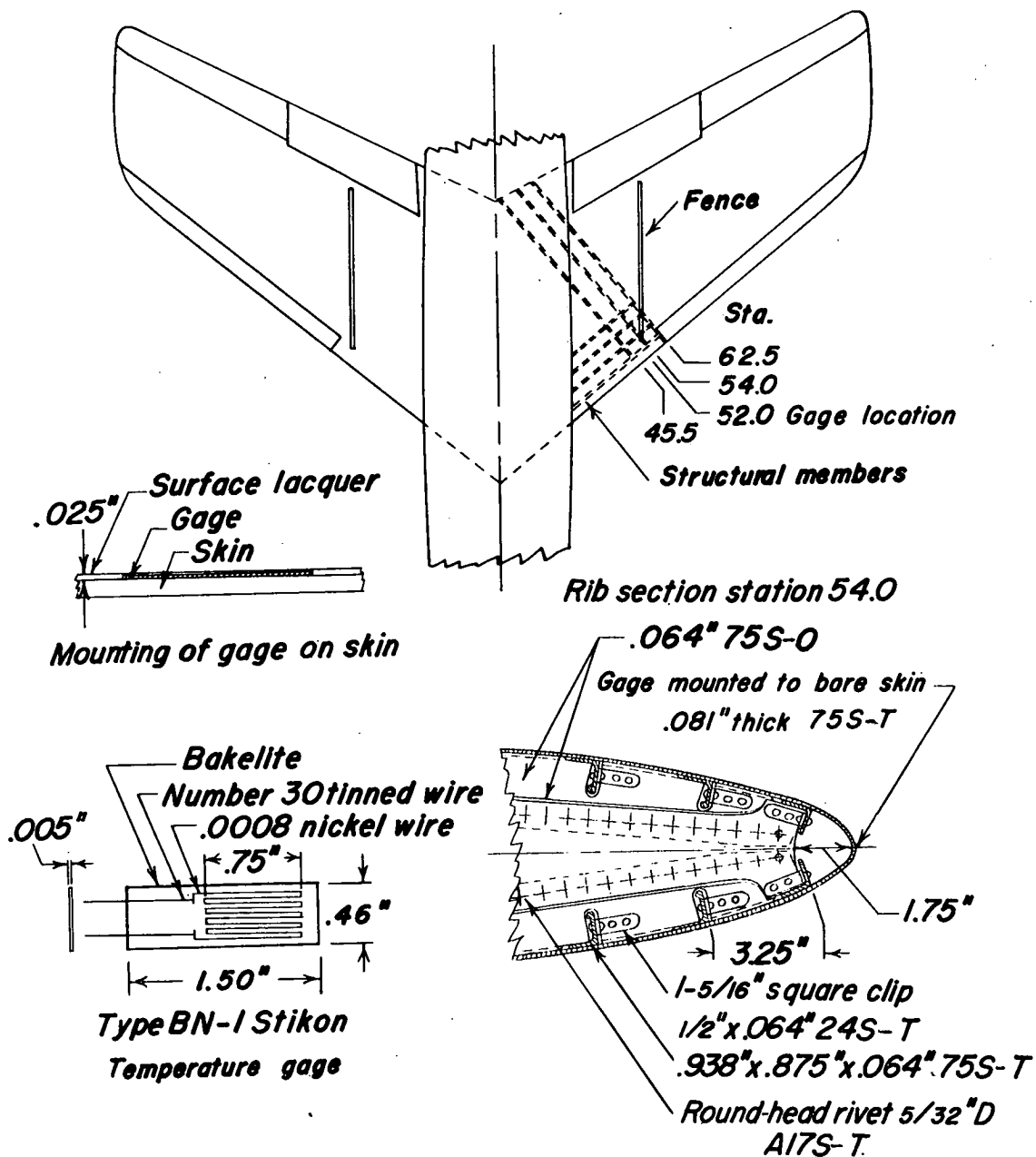


Figure 5.- Position of wing-temperature gage.





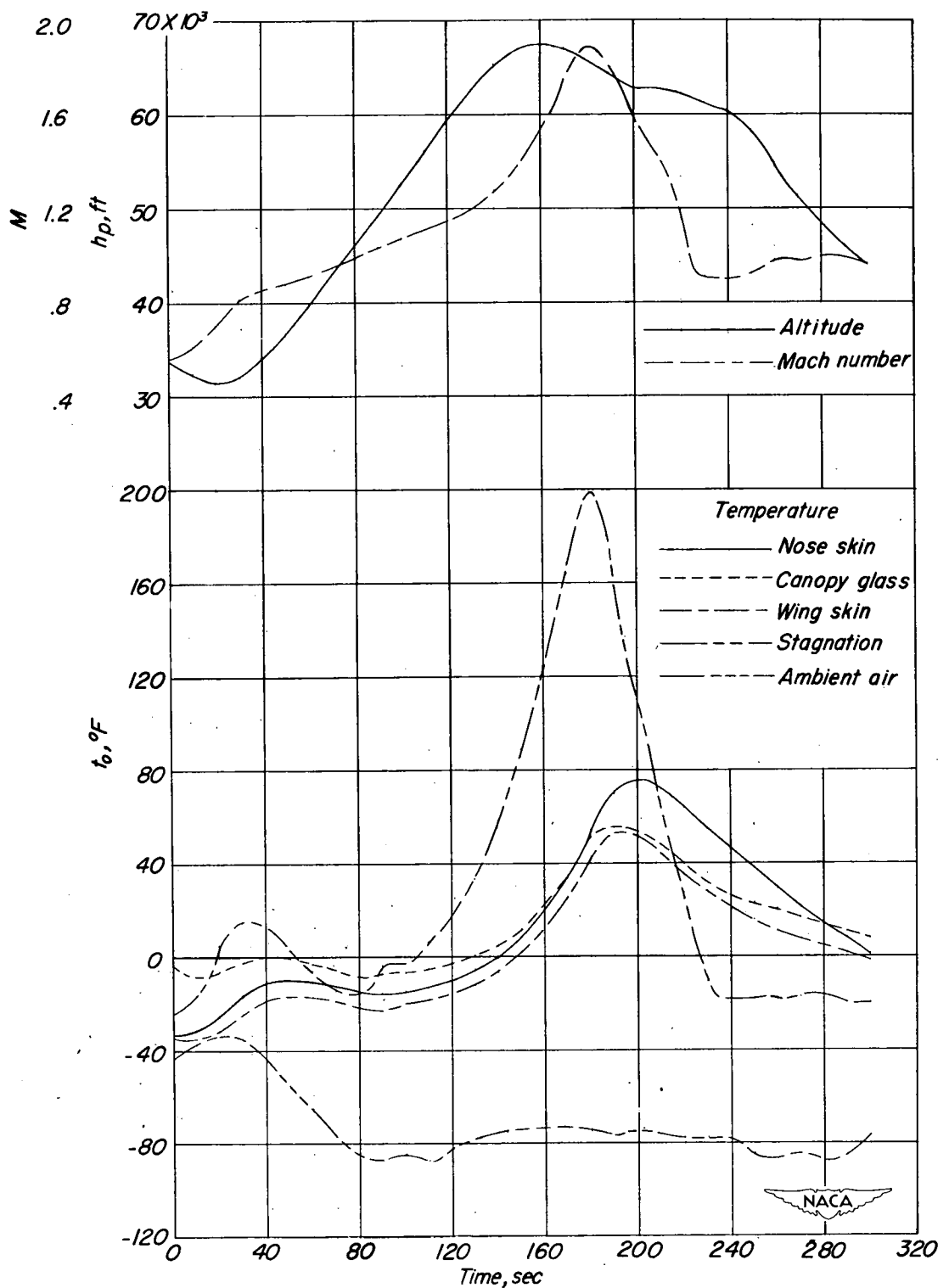


Figure 6.- Time history of pressure altitude, Mach number, and temperature during a flight of the Douglas D-558-II airplane to maximum Mach number.

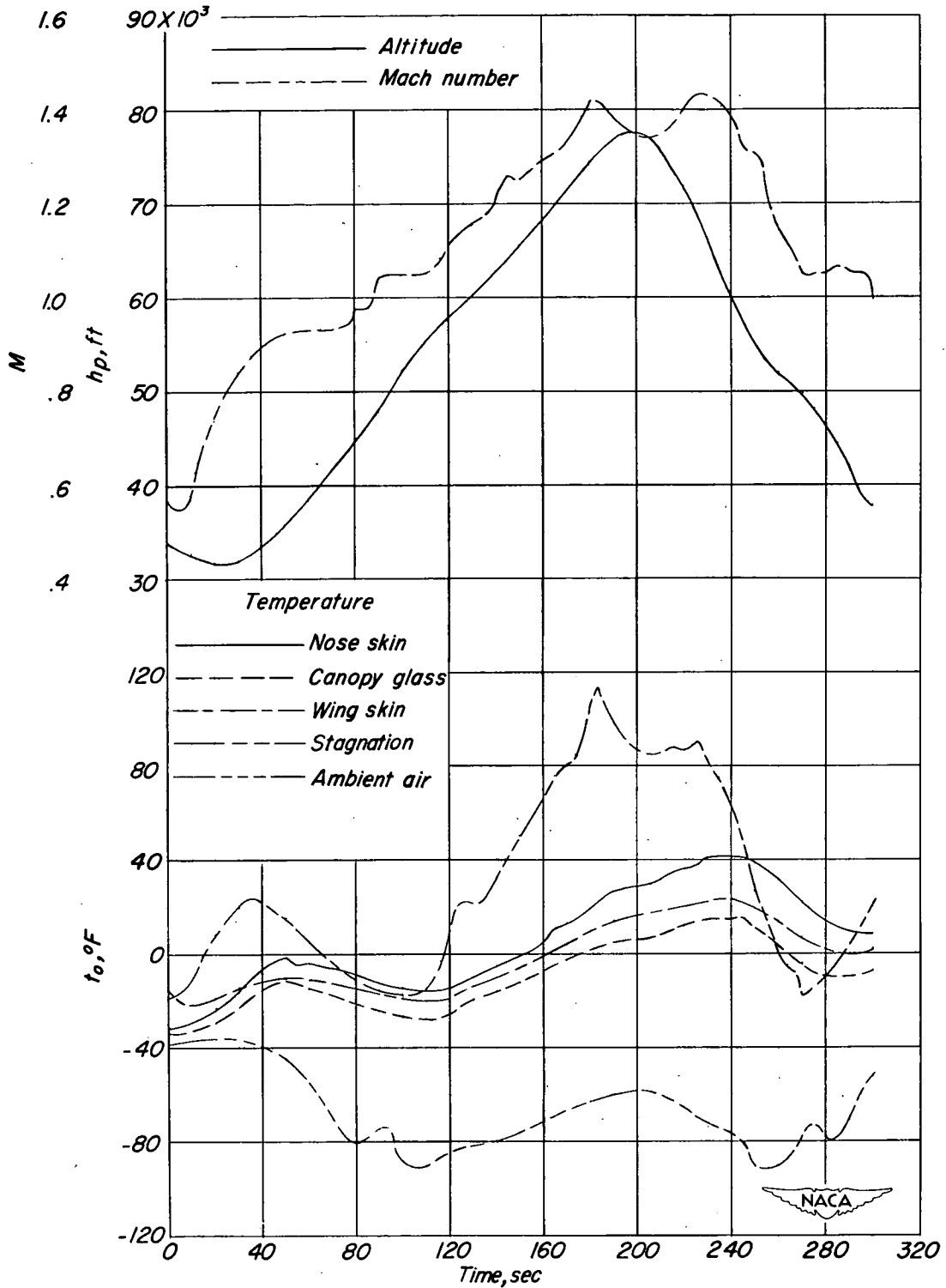


Figure 7.- Time history of pressure altitude, Mach number, and temperature during a flight of the Douglas D-558-II airplane to maximum altitude.

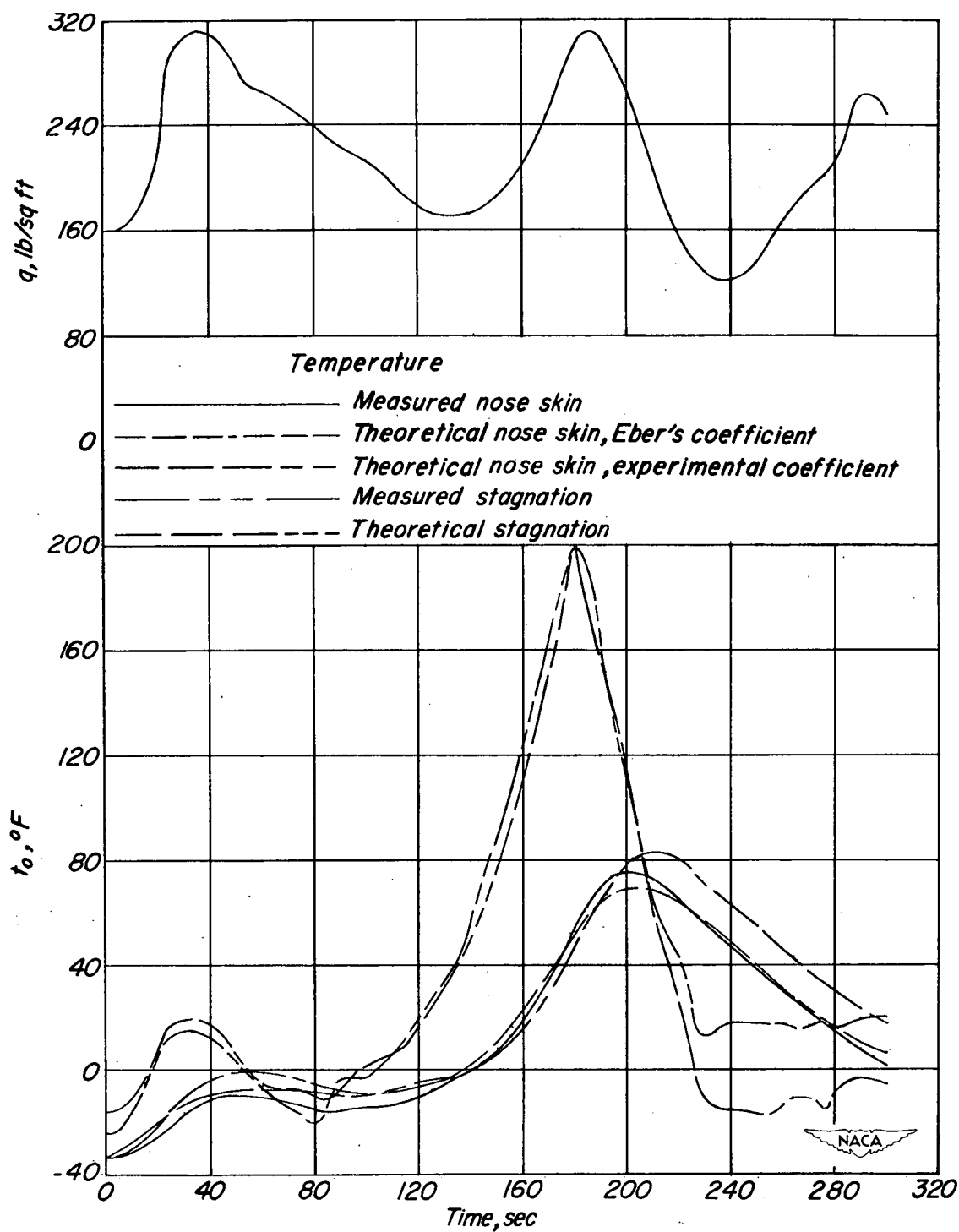


Figure 8.- Time history of measured and theoretical stagnation and nose-skin temperature and dynamic pressure during a flight to maximum Mach number.

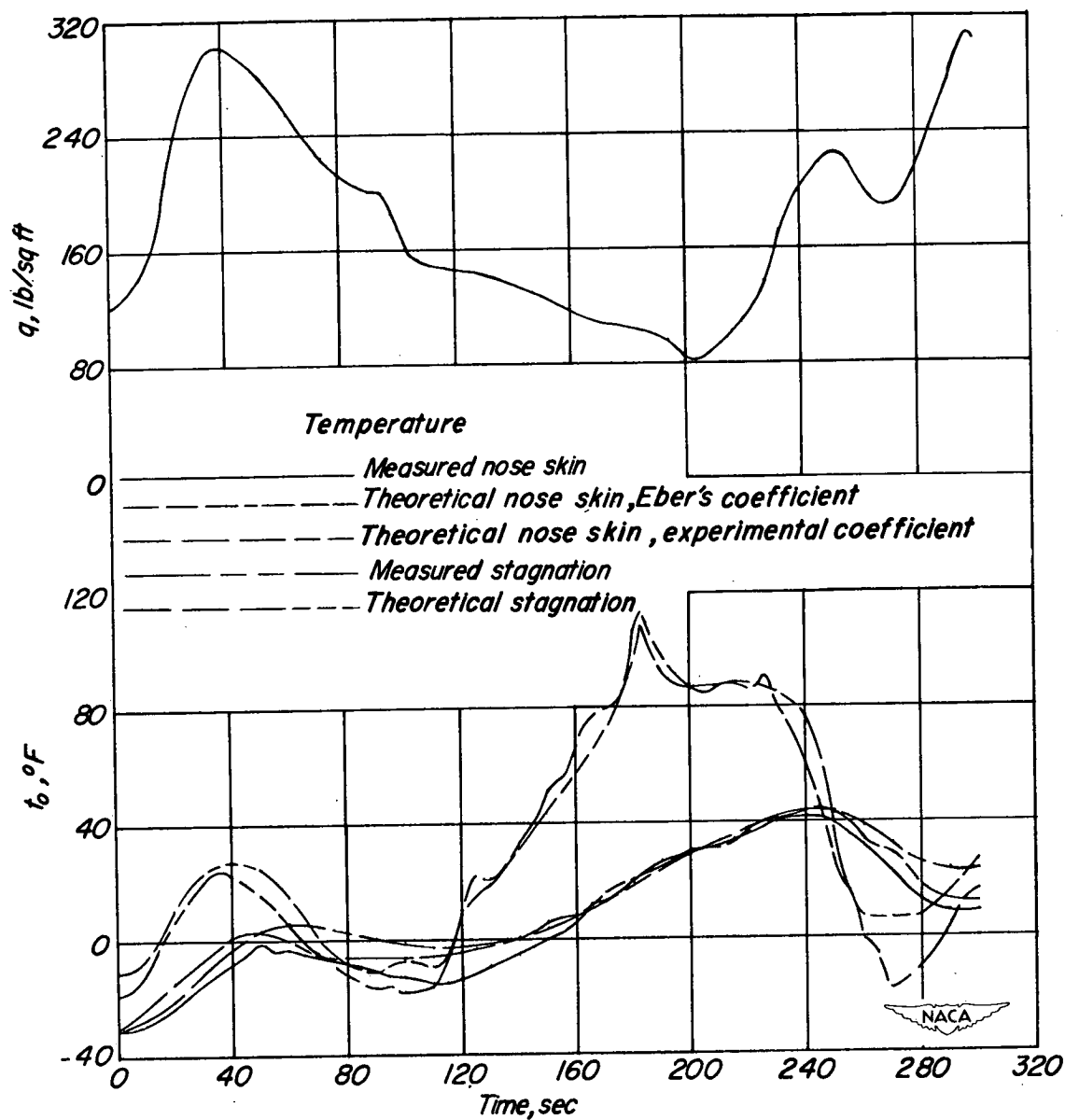


Figure 9.- Time history of measured and theoretical stagnation and nose-skin temperature and dynamic pressure during a flight to maximum altitude.